Advances in Nanoparticles, 2016, 5, 114-122
Published Online February 2016 in SciRes. http://www.scirp.org/journal/anp
http://dx.doi.org/10.4236/anp.2016.51013

Synthesis and Characterisation of In_2O_3 Nanoparticles from *Astragalus gummifer*

Kanchana Latha Chitturi[1], Aparna Yaramma[1*], Ramchander Merugu[2], Ravinder Dachepalli[3], Jaipal Kandhadi[4]

[1]Department of Physics, JNTUH, CEH, Kukatpally, Hyderabad, India
[2]Department of Bio Chemistry, Mahatma Gandhi University, Nalgonda, India
[3]Department of Physics, Osmania University, Hyderabad, India
[4]Inorganic and Physical Chemistry Division, Indian Institute of Chemical Technology, Hyderabad, India
Email: *yarrama@yahoo.com

Received 21 October 2015; accepted 20 February 2016; published 23 February 2016

Abstract

Exploitation of green chemistry approach for the synthesis of Indium Oxide nanoparticles using green synthesis has received a great attention in the field of nanotechnology. To demonstrate a biogenic method that involves the Katira gum (*Astragalus gummifer*) leading to the formation of different morphological In_2O_3 using the precursor Indium (III) Acetylacetonate and TG-DTA is characterised for calcination temperature and it is found to be above 500˚C. Different techniques such as XRD, UV-VIS, SEM and EDAX have been used for the characterisation of In_2O_3 nanoparticles. The average crystallite size of Indiumoxide nanoparticles is determined as 19 nm by using Scherrer's Equation and PSA and studying optical properties.

Keywords

In_2O_3 Nanoparticles, Bio Synthesis, XRD, UV-Vis, SEM and EDAX, PSA, RAMAN FTIR and PL

1. Introduction

These days nanotechnology is one of the important research fields. For several years, scientists have constantly explored different bio synthetic methods to synthesize nanoparticles. The gum mediated synthesis of nanoparticles is eco friendly, efficient and easier when compared to chemical mediated or microbe mediated synthesis. For the production of nanoparticles plant extract is an alternative method to chemical and physical methods and it eliminates the elaborate process of maintaining cell cultures.

*Corresponding author.

How to cite this paper: Chitturi, K.L., Yaramma, A., Merugu, R., Dachepalli, R. and Kandhadi, J. (2016) Synthesis and Characterisation of In_2O_3 Nanoparticles from *Astragalus gummifer*. *Advances in Nanoparticles*, **5**, 114-122.
http://dx.doi.org/10.4236/anp.2016.51013

Among the many transparent conducting oxide materials like SnO_2, Indium oxide is physically stable chemically inert and hence it is superior for applications in several aspects. Usually, Indium oxide crystallizes into a cubic bixbyite structure with a melting point temperature of 1910˚C. It is highly conductive and exhibits a direct band gap between 3.55 and 3.75 eV, which is an unusual property for wide band gap material. Indium Oxide also has very interesting optical properties. It absorbs IR light waves beyond 900 nm and transmits visible light of wave length 400 to 700 nm. It has interesting properties such as high transparency to high electrical conductance, visible light and strong interaction between certain poisonous gas molecules and its surfaces [1]-[3]. Indium Oxide with these properties makes an interesting material for various applications, including solar cells [1] [2], Panel Displays [4], Organic Light Emitting Diodes [5], Photo Catalysts [6], Architectural Glasses [7], Field Emission [8]. Moreover, Indium Oxide is an important material for Semiconductor Gas Sensors [9]-[14]. Recently, investigations on preparation of Indium Oxide nano structures with various forms such as Nantubes [15], Nanobelts [16]-[18], Nanofibers [19] [20], Nanowires [5] [8] [21]-[26] and Nanoparticles [27]-[29] have been widely emphasised to extend their technological usages. Nanoparticulate form of Indium Oxide nanostructures has been used as a promising material for gas sensor applications. Tragacanth is a natural gum (Botanical name *Astragalus gummifer*) obtained from the dried sop of several species of Middle Eastern legumes of the genus *Astragalus*. It is tasteless, odourless and viscous and is obtained from the root of the plant and dried. The gum comes from a thorny shrub. It has been used as treatment for burns, cough, texturant additive and also as a binder to hold all the powdered herbs together.

2. Experimental

For the preparation of Indium Oxide nanoparticles, the chemical materials used were Indium (III) Acetylacetonate (99.99+% purity, Sigma Aldrich) and *Astragalus gummifer* (Katira Gum) bought from local Unani (*davaasaas*) Shop. The *Astragalus gummifer* (0.05 gm) and Indium (III) Acetylacetonate (0.4 gm) were mixed and crushed into fine powder using mortar and pistle. The precursor was characterised by TG-DTA to determine the calcination temperature and is found to be above 450˚C (**Figure 2**). Then the precursor was calcined in box furnace at 500˚C for 2 hours in air. The yellowish nano-powder of In_2O_3 as described in (**Figure 1**) was obtained.

Physical Characterization

The precursor was characterised by TG-DTA (HITACHI Spectrophotometer) to determine the thermal decomposition and crystallite temperature was found to be at 500˚C (**Figure 2**). The dried precursor was ground and

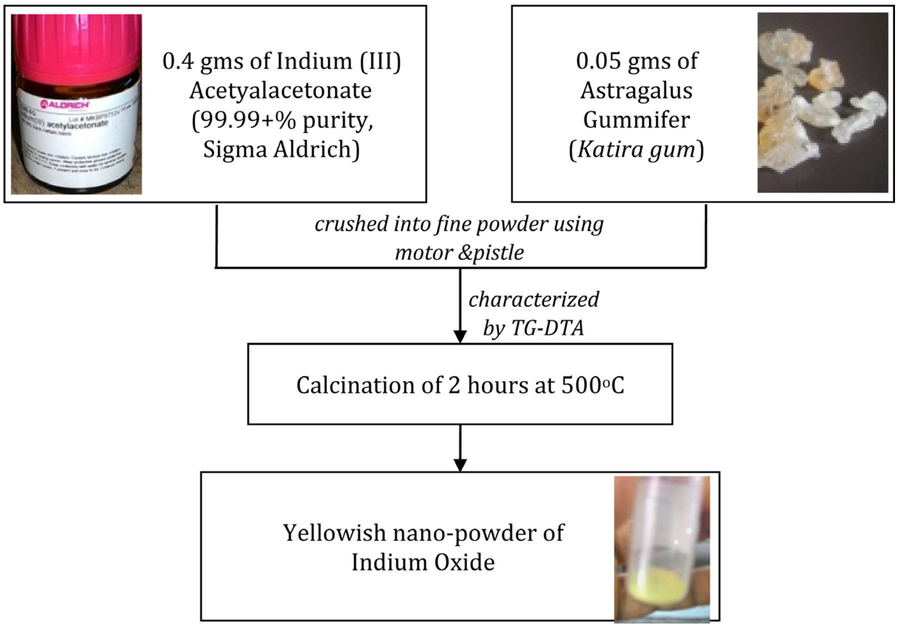

Figure 1. Flow chart of preparation of In_2O_3 nanoparticles.

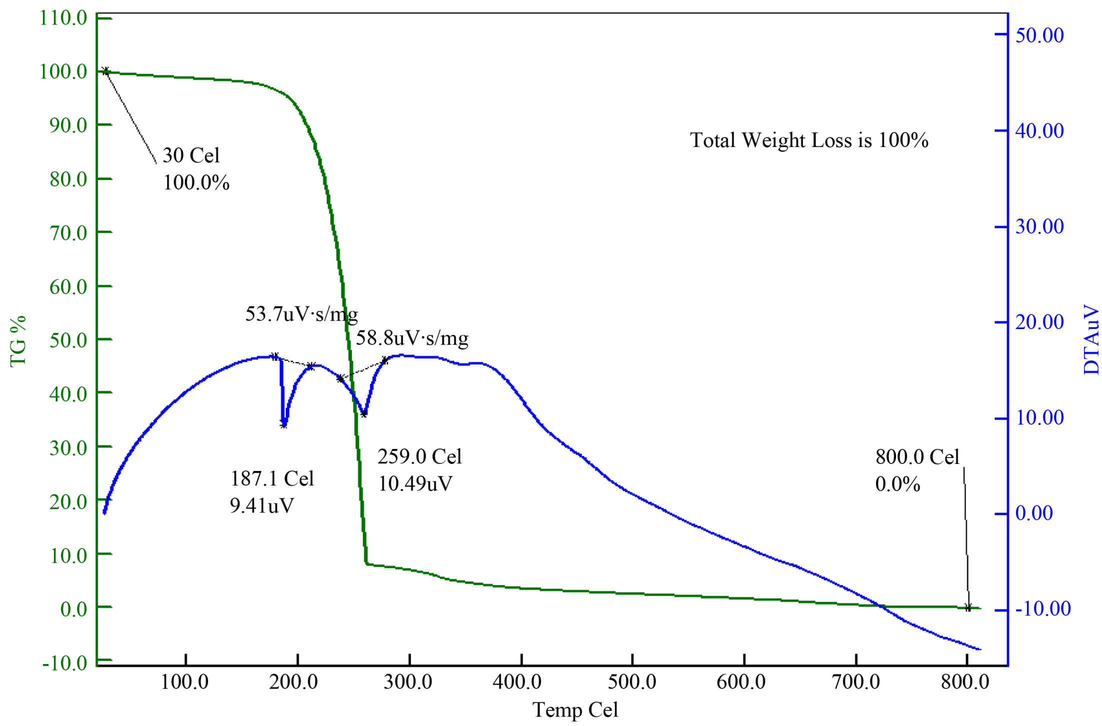

Figure 2. TG-DTA curves of thermal decompositia of In_2O_3 precursorat a heating rate of 10˚C/min in static air.

subsequently calcined in box furnace at 500˚C for 2 hours in air. The dried precursor and calcined samples of In_2O_3 were characterised for crystal phase identification by powder XRD using with Cuk$_\alpha$ radiation (λ = 0.15406 nm). The optical absorption spectra were measured in the range of 200 - 800 nm using UV-Vis scanning spectrometer. Photo Luminiscence (PL) measurement was carried on a luminescence spectrometer with xenon lamp as the excitation source at 25˚C temperature. The samples were dispersed in using ethanol and the excitation wave length used in PL measurement was 353 nm.

3. Results & Discussion

3.1. TG-DTA Analysis

The TG-DTA analysis curves of as prepared In_2O_3 precursor are shown in **Figure 2**. The TG curve in **Figure 2** shows a major weight loss step from 200˚C up to about 350˚C. The major weight loss is due to the combustion of organic matter (CO and OH groups) present in the precursor and slight weight loss (combustion of remaining carbonyl group) was observed at 470˚C. On the DTA curve (**Figure 2**) a main exothermic effect was observed between 300˚C and 400˚C with maximum at about 320˚C indicating that the thermal events can be due to the burning of organic species in the precursor powders from the amorphous component.

3.2. XRD Analysis

The formation of nano crystalline In_2O_3 as decomposition product was confirmed by XRD pattern in **Figure 3**. All of the detectable peaks (**Figure 3**) can be indexed as the In_2O_3 cubic structure in the Standard Data (JCPDS: 06-0416). The cubic lattice parameter "*a*" can be calculated from the XRD spectra is 10.222 Å which is close to those of lattice constants α = 0.32488 nm and C = 0.52066 nm in the Standard Data (JCPDS: 06-0416). The crystallite sizes of the powders were estimated from X-ray line broadening using Scherrer's Equation [30] (*i.e.*, $D = 0.89\lambda/\beta \text{Cos}\theta$), where λ is the wavelength of the X-ray radiation, k is a constant taken as 0.89, 2θ is the diffraction angle (30.286˚), β is the Full Width at Half Maximum (FWHM = 0.4723) and is obtained to be 19.25 nm for In_2O_3 sample calcined at 500˚C. The particle size and lattice parameter of In_2O_3 sample is summarised in **Table 1**.

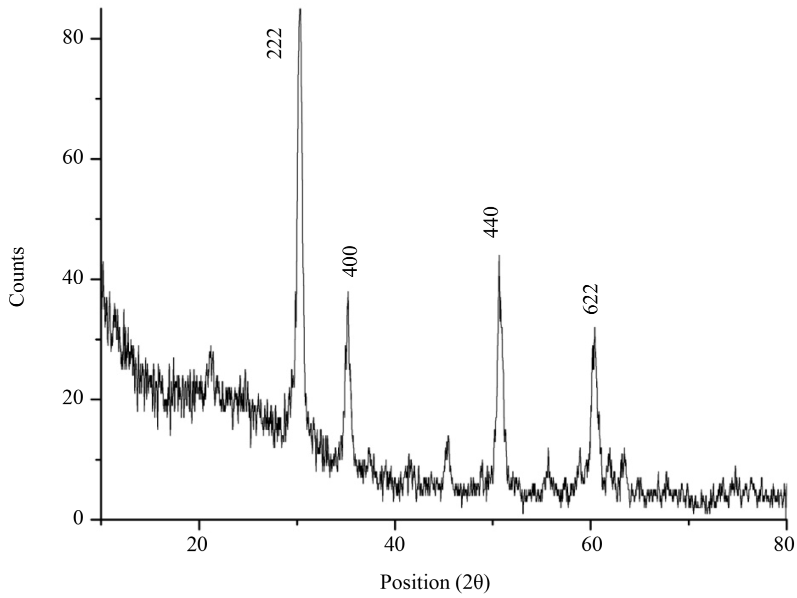

Figure 3. XRD pattern of nano crystalline In_2O_3 sample calcined in air for 2 hours at 500˚C.

Table 1. In_2O_3 nano crystalline sample from different characterisations data.

Average Particle size (nm) from XRD	Cubic lattice parameter a (nm)	Morphology from SEM	Estimated Band gap UV	Estimated Band gap PL	PSA	EDAX Atomic %	EDAX Weight %
19.25 nm	1.0222 nm	Spherical	3.86 eV	3.51 eV	24 nm	O/In = 2.2	93

3.3. EDAX & SEM Analysis

The SEM images in **Figure 4** showed that the In_2O_3 nanoparticles are formed as cubic crystals. However, the particle size as well as agglomeration increased and the smaller grains coalesced to form larger size particles [31]. The EDAX data at 500˚C sintering temperature suggested the stoichiometry of In_2O_3 nanoparticles with the elemental composition of oxygen and Indium and their atomic and weight percentages are given **Table 1**. The atomic ratio of (O/In) calculated as 2.2 indicated the stoichiometric composition of In_2O_3 which is in good agreement with the theoretical value of 1.5.

3.4. PSA Analysis

The average particle size of the In_2O_3 nanoparticle from the particle size analyzer, as in **Figure 5**, was found to be 24 nm as shown in **Table 1**.

3.5. RAMAN Studies

The In_2O_3 Raman spectrum (**Figure 6**) shows the expected vibrational modes at 109,475 cm^{-1}, which in turn is an unambiguous signature of the cubic In_2O_3 structure [32]. The higher frequency (1500 cm^{-1}) is due to super position of the contribution of the In-O vibration modes with frequency 630 cm^{-1}. The intensity peaks which are known to be related to the pure In_2O_3 vibrational modes which confirm the In_2O_3 cubic like feature.

3.6. FTIR Analysis

The IR spectra of In_2O_3 indicating that the bands around 3506 cm^{-1} and 1623 cm^{-1} are attributed to the absorptions of hydroxyls from absorbed water or alcohols and those at 1416 cm^{-1} can be ascribed to the C-H vibrations of the organics in **Figure 7**. The band at 1050 cm^{-1} is due to C-O vibrations. While the absorptions around 1500 cm^{-1} are due to the In-O vibrations [33]. The weak absorption at 1568 cm^{-1} is due to C-O vibrations from the

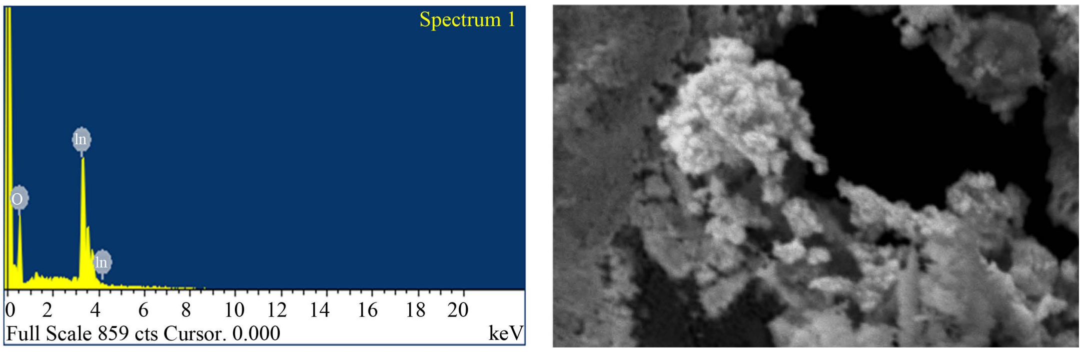

Figure 4. EDAX & SEM images of the nano crystalline In_2O_3 sample.

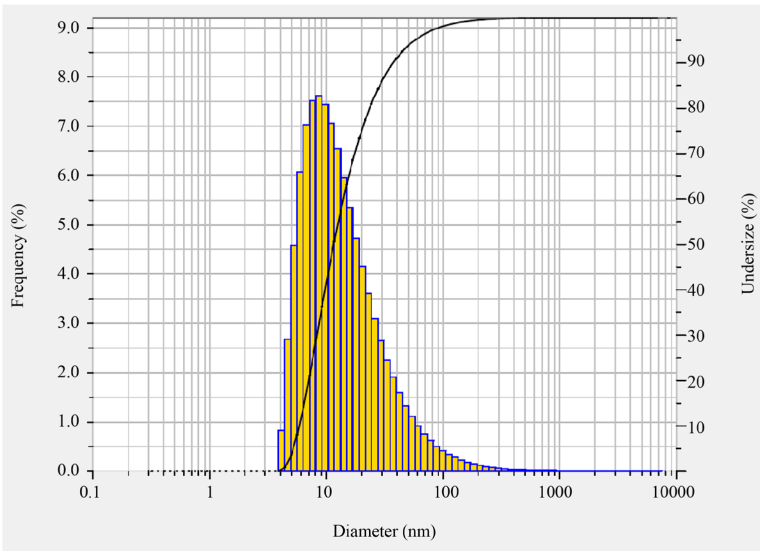

S.P. Area Ratio	Mean	S.D.	Mode
1.00	24.3 nm	11.3 nm	17.9 nm

Figure 5. Particle size analysis of the nano crystalline In_2O_3 sample.

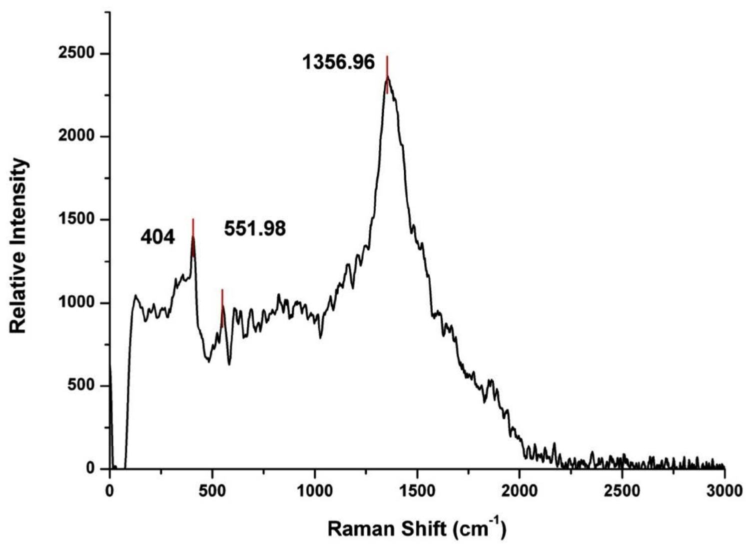

Figure 6. Raman Spectra of nanocrystalline In_2O_3 sample calcined in air for 2 hours at 500˚C.

Acetylacetone species [34]. The results indicate the presence of few acetyl acetone species on the surface species of the In_2O_3 nanocrystals.

3.7. UV-Vis Absorbance

Now let us consider the optical properties of the In_2O_3 samples. The UV-visible absorption spectra of all the In_2O_3 samples (**Figure 8**) exhibit a strong absorption below 450 nm (2.7 eV) with a well defined absorbance peak at around 320 nm (3.88 eV). This value is greater than that of 3.6 eV for the In_2O_3 reported in the literature [2].

3.8. PL Spectrum

Figure 9 shows the room temperature PL spectra of the nanocrystalline In_2O_3 samples measured using a

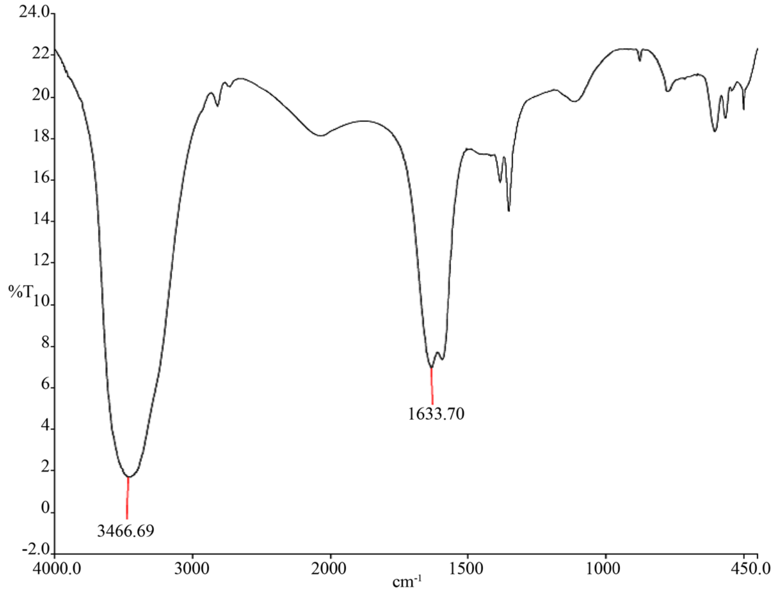

Figure 7. FTIR nano-crystalline In_2O_3 sample calcined in air at 500˚C.

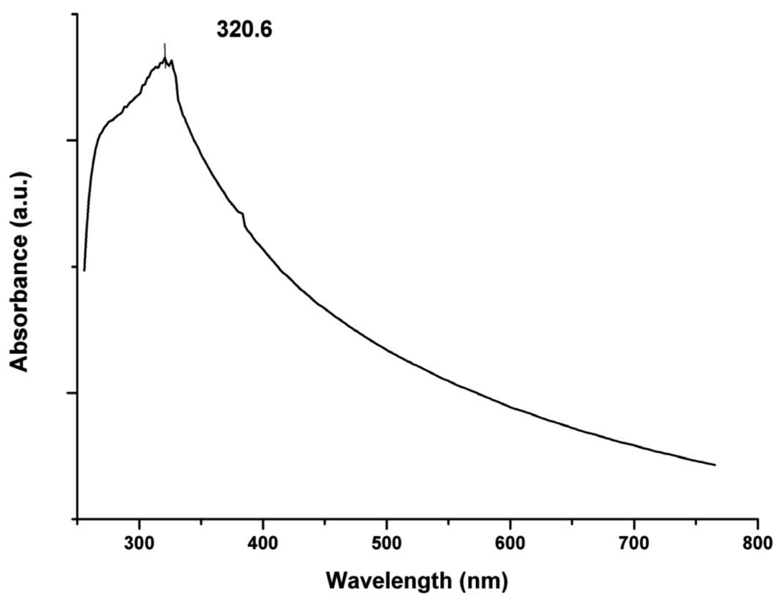

Figure 8. Room temperature optical absorbance spectra of nano crystalline In_2O_3 sample calcined in air for 2 hours at 500˚C.

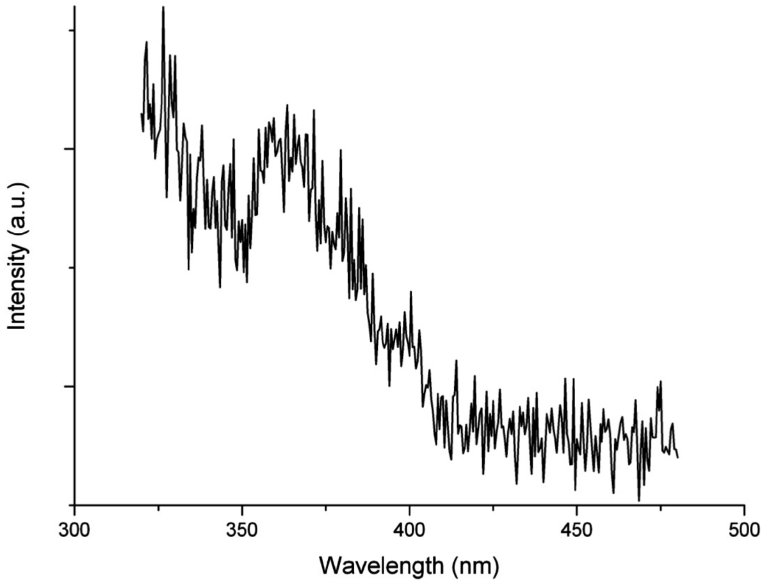

Figure 9. Room temperature photo luminescence spectra of the synthesized nano crystalline In_2O_3 sample calcined in air for 2 hours at 500˚C.

Xenon laser of 270 nm as an excitation source. The spectra of all the samples mainly consist of a strong UV emission broad band having emission maximum at ~353 nm (3.51 eV). It is well known that the bulk In_2O_3 cannot emit light at room temperature [38]. However PL emissions of our nano crystalline In_2O_3 samples are possibly due to the effect of the oxygen vacancies as reported in literatures [14] [17] [19] [20] [27] [28] [36]-[38]. In the present work, oxygen vacancies would generally act as deep defect donors and cause the formation of new energy levels in the band gap of In_2O_3 samples. Thus the PL emission from In_2O_3 nanoparticles results from the radiative recombination of electron occupying oxygen vacancies with a photo excited hole which is analogous to the photo luminescence mechanism of ZnO and SnO_2 semi conductors [19] [38].

4. Conclusion

We have synthesized nanoparticles of In_2O_3 by a green method using *Astragalus gummifer*. Structural, morphological chemical composition and optical properties of the green synthesized nanoparticles were characterised. XRD, RAMAN, SEM analysis showed that the In_2O_3 samples were cubic with particle size of 19 nm. The morphology and size of In_2O_3 materials were affected by the calcination temperature. The prepared In_2O_3 nanoparticles showed a strong PL emission in the UV region. The strong emissions of In_2O_3 are attributed to the radiative recombination of electron occupying oxygen vacancies with a photo excited hole.

References

[1] Hamburg, I. and Granqvist, C.G. (1986) Evaporated Sn-Doped In_2O_3 Films: Basic Optical Properties and Applications to Energy-Efficient Windows. *Journal of Applied Physics*, **60**, R123. http://dx.doi.org/10.1063/1.337534

[2] Granqvist, C.G. (1993) Transparent Conductive Electrodes for Electrochromic Devices: A Review. *Applied Physics A*: *Solid-State Ionics*, **57**, 19-24. http://dx.doi.org/10.1007/BF00331211

[3] Gopchandran, K.G., Joseph, B., Abraham, J.T., Koshy, P. and Vaidyan, V.K. (1997) The Preparation of Transparent Electrically Conducting Indium Oxide Films by Reactive Vacuum Evaporation. *Vacuum*, **48**, 547-550. http://dx.doi.org/10.1016/S0042-207X(97)00023-7

[4] Zhang, Y., Ago, H., Liu, J., Yumura, M., Uchida, K., Ohshima, S., Iijima, S., Zhu, J. and Zhang, X. (2004) The Synthesis of In, In_2O_3 Nanowires and In_2O_3 Nanoparticles with Shape-Controlled. *Journal of Crystal Growth*, **264**, 363-368. http://dx.doi.org/10.1016/j.jcrysgro.2004.01.025

[5] Lao, J., Huang, J., Wang, D. and Ren, Z.F. (2004) Self-Assembled In_2O_3 Nanocrystal Chains and Nanowire Networks. *Advanced Materials*, **16**, 65-69. http://dx.doi.org/10.1002/adma.200305684

[6] Zhu, H., Wang, N., Wang, L., Yao, K. and Shen, X. (2005) *In Situ* X-Ray Diffraction Study of the Phase Transition of

Nanocrystalline In(OH)$_3$ to In_2O_3. *Inorganic Materials*, **41**, 609-612. http://dx.doi.org/10.1007/s10789-005-0178-x

[7] Chen, X., Zhang, Z., Zhang, X., Liu, J. and Qian, Y. (2005) Single-Source Approach to the Synthesis of In_2S_3 and In_2O_3 Crystallites and Their Optical Properties. *Chemical Physics Letters*, **407**, 482-486. http://dx.doi.org/10.1016/j.cplett.2005.03.141

[8] Kar, S., Chakrabarti, S. and Chaudhuri, S. (2006) Morphology Dependent Field Emission from In_2O_3 Nanostructures. *Nanotechnology*, **17**, 3058. http://dx.doi.org/10.1088/0957-4484/17/12/041

[9] Gurlo, A., Ivanovskaya, M., Barsan, N., Shweizer-Berberich, M., Weimar, U., Gopel, W. and Dieguez, A. (1997) Grain Size Control in Nanocrystalline In_2O_3 Semiconductor Gas Sensors. *Sensors and Actuators B*: *Chemical*, **44**, 327-333. http://dx.doi.org/10.1016/S0925-4005(97)00199-8

[10] Comini, E., Cristalli, A., Faglia, G., Sberveglieri, G. (2000) Light Enhanced Gas Sensing Properties of Indium Oxide and Tin Dioxide Sensors. *Sensors and Actuators B*: *Chemical*, **65**, 260-263. http://dx.doi.org/10.1016/S0925-4005(99)00350-0

[11] Steffes, H., Imawan, C., Solzbacher, F. and Obermeier, E. (2000) Fabrication Parameters and NO_2 Sensitivity of Reactively RF-Sputtered In_2O_3 Thin Films. *Sensors and Actuators B*: *Chemical*, **68**, 249-253. http://dx.doi.org/10.1016/S0925-4005(00)00437-8

[12] Ivanovskaya, M., Gurlo, A. and Bogdanov, P. (2001) Mechanism of O_3 and NO_2 Detection and Selectivity of In_2O_3 Sensors. *Sensors and Actuators B*: *Chemical*, **77**, 264-267. http://dx.doi.org/10.1016/S0925-4005(01)00708-0

[13] Gurlo, A., Barson, N., Weimar, U., Ivanovskaya, M., Tuarino, A. and Siciliano, P. (2003) Polycrystalline Well-Shaped Blocks of Indium Oxide Obtained by the Sol-Gel Method and Their Gas-Sensing Properties. *Chemistry of Materials*, **15**, 4377-4383. http://dx.doi.org/10.1021/cm031114n

[14] Tang, Q., Zhou, W., Zhang, W., Ou, S., Jiang, K., Yu, W. and Qian, Y. (2005) Size-Controllable Growth of Single Crystal In(OH)$_3$ and In_2O_3 Nanocubes. *Crystal Growth & Design*, **5**, 147-150. http://dx.doi.org/10.1021/cg049914d

[15] Shen, X.-P., Liu, H.-J., Fan, Z., Jiang, Y., Hong, J.-M. and Xu, Z. (2005) Construction and Photoluminescence of In_2O_3 Nanotube Array by CVD-Template Method. *Journal of Crystal Growth*, **276**, 471-477. http://dx.doi.org/10.1016/j.jcrysgro.2004.11.394

[16] Chen, H.J., Choi, Y.S., Bae, S.Y. and Park, J. (2005) Bicrystalline Indium Oxide Nanobelts. *Applied Physics A*, **81**, 539-542. http://dx.doi.org/10.1007/s00339-004-2898-1

[17] Jeong, J.S., Lee, J.Y., Lee, C.J., An, S.J. and Yi, G.-C. (2004) Synthesis and Characterization of High-Quality In_2O_3 Nanobelts via Catalyst-Free Growth Using a Simple Physical Vapor Deposition at Low Temperature. *Chemical Physics Letters*, **384**, 246-250. http://dx.doi.org/10.1016/j.cplett.2003.12.027

[18] Gao, T. and Wang, T. (2006) Catalytic Growth of In_2O_3 Nanobelts by Vapor Transport. *Journal of Crystal Growth*, **290**, 660-664. http://dx.doi.org/10.1016/j.jcrysgro.2006.01.046

[19] Liang, C.H., Meng, G.W., Lei, Y., Phillipp, F. and Zhang, L.D. (2001) Catalytic Growth of Semiconducting In_2O_3 Nanofibers. *Advanced Materials*, **13**, 1330-1333. http://dx.doi.org/10.1002/1521-4095(200109)13:17<1330::AID-ADMA1330>3.0.CO;2-6

[20] Zhang, Y., Li, J., Li, Q., Zhu, L., Liu, X., Zhong, X., Meng, J. and Cao, X. (2007) Preparation of In_2O_3 Ceramic Nanofibers by Electrospinning and Their Optical Properties. *Scripta Materialia*, **56**, 409-412. http://dx.doi.org/10.1016/j.scriptamat.2006.10.032

[21] Peng, X.S., Wang, Y.W., Zhang, J., Wang, X.F., Zhao, L.X., Meng, G.W. and Zhang, L.D. (2002) Large-Scale Synthesis of In_2O_3 Nanowires. *Applied Physics A*, **74**, 437-439. http://dx.doi.org/10.1007/s003390101037

[22] Wu, X.C., Hong, J.M., Han, Z.J. and Tao, Y.R. (2003) Fabrication and Photoluminescence Characteristics of Single Crystalline In_2O_3 Nanowires. *Chemical Physics Letters*, **373**, 28-32. http://dx.doi.org/10.1016/S0009-2614(03)00582-7

[23] Kam, K., Deepak, F.L., Cheetham, A.K. and Rao, C.N.R. (2004) In_2O_3 Nanowires, Nanobouquets and Nanotrees. *Chemical Physics Letters*, **297**, 329-334. http://dx.doi.org/10.1016/j.cplett.2004.08.129

[24] Zhang, Y., Ago, H., Liu, J., Yumura, M., Uchida, K., Ohshima, S., Iijima, S., Zhu, J. and Zhang, X. (2004) The Synthesis of In, In_2O_3 Nanowires and In_2O_3 Nanoparticles with Shape-Controlle. *Journal of Crystal Growth*, **264**, 363-368. http://dx.doi.org/10.1016/j.jcrysgro.2004.01.025

[25] Li, S.Q., Liang, Y.X. and Wang, T.H. (2006) Nonlinear Characteristics of the Fowler-Nordheim Plot for Field Emission from Nanowires Grown on InAs Substrate. *Applied Physics Letters*, **88**, Article ID: 053107. http://dx.doi.org/10.1063/1.2159092

[26] Cheng, G., Stren, E., Guthrie, S., Reed, M.A., Klin, R., Hao, Y., Meng, G. and Zhang, L. (2006) Indium Oxide Nanostructures. *Applied Physics A*, **85**, 233-240. http://dx.doi.org/10.1007/s00339-006-3706-x

[27] Murali, A., Barve, A., Leppert, V.L. and Risbud, S.H. (2001) Synthesis and Characterization of Indium Oxide Nanoparticles. *Nano Letters*, **1**, 287-289. http://dx.doi.org/10.1021/nl010013q

[28] Seo, W.S., Jo, H.H., Lee, K. and Park, J.T. (2003) Preparation and Optical Properties of Highly Crystalline, Colloidal, and Size-Controlled Indium Oxide Nanoparticles. *Advanced Materials*, **15**, 795-797. http://dx.doi.org/10.1002/adma.200304568

[29] Zhan, Z., Song, W. and Jiang, D. (2004) Preparation of Nanometer-sized In_2O_3 Particles by a Reverse Microemulsion Method. *Journal of Colloid and Interface Science*, **271**, 366-371. http://dx.doi.org/10.1016/j.jcis.2003.11.048

[30] Cullity, B.D. and Stock, S.R. (2001) Elements of X-Ray Diffraction. 3rd Edition, Prentice Hall, New Jersey.

[31] Chandran, S.P., Chaudhary, M., Pasricha, R., Ahmad, A. and Sastry, M. (2006) Synthesis of Gold Nanotriangles and Silver Nanoparticles Using Aloe Vera Plant Extract. *Biotechnology Progress*, **22**, 577-583. http://dx.doi.org/10.1021/bp0501423

[32] Sobotta, H., Neumann, H., Kiin, G. and Riede, V. (1990) Infrared Lattice Vibrations of In_2O_3. *Crystal Research and Technology*, **25**, 61-64. http://dx.doi.org/10.1002/crat.2170250112

[33] Ho, W.H. and Yen, S.K. (2006) Preparation and Characterization of Indium Oxide Film by Electrochemical Deposition. *Thin Solid Films*, **498**, 80-84. http://dx.doi.org/10.1016/j.tsf.2005.07.072

[34] Chu, D.W., Zeng, Y.P., Jiang, D.L. and Xu, J.Q. (2007) Tuning the Phase and Morphology of In_2O_3 Nanocrystals via Simple Solution Routes. *Nanotechnology*, **18,** 435605-435610. http://dx.doi.org/10.1088/0957-4484/18/43/435605

[35] Ohhata, Y., Shinoki, F. and Yoshida, S. (1979) Optical Properties of R.F. Reactive Sputtered Tin-Doped In_2O_3 Films. *Thin Solid Films*, **59**, 255-261. http://dx.doi.org/10.1016/0040-6090(79)90298-0

[36] Lee, M.S., Choi, W.C., Kim, E.K., Kim, C.K. and Min, S.K. (1996) Characterization of the Oxidized Indium Thin Films with Thermal Oxidation. *Thin Solid Films*, **279**, 1-3. http://dx.doi.org/10.1016/0040-6090(96)08742-1

[37] Zhou, H.J., Cai, W.P. and Zhang, L.D. (1999) Photoluminescence of Indium-Oxide Nanoparticles Dispersed within Pores of Mesoporous Silica. *Applied Physics Letters*, **75**, 495. http://dx.doi.org/10.1063/1.124427

[38] Zhang, J., Qing, X., Jiang, F. and Dai, Z. (2003) A Route to Ag-Catalyzed Growth of the Semiconducting In_2O_3 Nanowires. *Chemical Physics Letters*, **371**, 311-316. http://dx.doi.org/10.1016/S0009-2614(03)00272-0